Including Spatial Correlations in the Statistical MIMO Radar Target Model

Mark T. Frankford, *Student Member, IEEE*, Joel T. Johnson, *Fellow, IEEE*, and Emre Ertin

***Abstract*—Previous studies of statistical MIMO radar detection performance have used a target model that consists of a large number of point scatterers located within a rectangular target area. These point scatterers have scattering amplitudes that are complex random variables and are spatially uncorrelated, so that the target is a white noise process in space. Spatial correlations are introduced into the target model in this paper, and the impact of these correlations on MIMO radar system detection performance is analyzed.**

***Index Terms*—Statistical MIMO rada.**

I. Introduction

SEVERAL recent publications have examined the potential advantages of multiple-input multiple-output (MIMO) radar systems, including their use in target detection and parameter estimation applications [1]–[6]. A MIMO radar system consists of M transmitters and N receivers. If the geometry of transmit and receive antennas in a MIMO radar system provides angular diversity in observations of a target, it has been shown that for sufficiently complex targets the MIMO radar system can provide benefits in target detection compared to a phased array system, as the impact of target radar cross section (RCS) variations with angle can be reduced.

Reference [1] utilizes a statistical target scattering model to analyze the performance of a MIMO system. This model consists of a finite rectangular area within which an infinite number of scatterers are contained whose amplitudes are independent and identically distributed (IID) random variables. A similar model using a finite number of spatially uncorrelated scatterers has also been presented [7]. This paper extends the target scattering model of [1] to include spatial correlations among the random scatters by introducing an azimuthally symmetric Gaussian covariance function with only a single new parameter, the correlation distance. Furthermore, a method is presented which uses this model to compute the detection performance of a MIMO system for any given transmitter/receiver geometry and varying levels of correlation in the target.

Received signal properties for the correlated scatterers target model are derived in Section II, and it is shown that introducing correlation can alter the bistatic scattering behavior of the target so that forward scattering becomes more prominent. The performance of the MIMO detector of [1] is then derived in Section IV, and an optimal detector for the spatially correlated target is also examined. Sample results for a fixed total received power are illustrated in Section V to show that MIMO detection performance degrades as the correlation of the target as increased.

II. Correlated Scattering Model

Following [1], a 2-D MIMO geometry is utilized, as illustrated in Fig. 1. The target considered is not range resolved, and a single amplitude and phase characterizes the measurement for each transmit/receive pair of antennas. It is also assumed that the range from each transmitter and receiver to the target is similar, so that the range dependence of the received power (as well as the transmitter power) can be neglected here and incorporated later as part of the system signal-to-noise ratio in Section IV. The rectangular target is of dimensions $\Delta X \times \Delta Y$, and is composed of an infinite number of random scatterers whose complex scattering amplitudes are given by $\Sigma(\gamma,\beta)$ where (γ,β) are the local coordinates relative to the center of the target (x_0, y_0). The vector $\vec{r}_q$ in Fig. 1 indicates the distance and direction from the qth transmitter to the center of the target, while the vector $\vec{r}_p$ indicates the direction and distance from the the center of the target to the pth receiver. The vectors $\vec{k}_q$ and $\vec{k}_p$ are defined identically, except that their amplitude is the electromagnetic wavenumber ($2\pi/\lambda$, where λ is the electromagnetic wavelength).

Using this model, the scattered field measured by the p^{th} receiver that results from the q^{th} transmitter (labeled α_{pq}) is a sum over all the individual scatterers of the target including appropriate phase delays:

$$\alpha_{pq} = \int_{-\frac{\Delta x}{2}}^{\frac{\Delta x}{2}} \int_{-\frac{\Delta y}{2}}^{\frac{\Delta y}{2}} \Sigma(\gamma,\beta) e^{-j\vec{k}_q\cdot(\vec{r}_q+\vec{r})} e^{-j\vec{k}_p\cdot(\vec{r}_p-\vec{r})} d\gamma d\beta \quad (1)$$

in which only $\vec{r}$ and Σ are functions of γ and β. The measurements of the MIMO system consist of MN α_{pq} values, which are grouped into the vector $\bar{\alpha}$.

If $\Sigma(\gamma,\beta)$ are described as zero-mean complex Gaussian random variables, then the vector $\bar{\alpha}$ is a zero-mean complex Gaussian vector ($\sim \mathcal{CN}(0,\boldsymbol{A})$) whose complete specification requires knowledge only of the covariance matrix $\boldsymbol{A} = E\{\bar{\alpha}\bar{\alpha}^H\}$. Computation of the covariance matrix elements

Manuscript received February 23, 2010; revised March 25, 2010.Date of publication April 12, 2010; date of current version April 28, 2010. The associate editor coordinating the review of this manuscript and approving it for publication was Prof. Andread Jakobsson.

M. T. Frankford and J. T. Johnson are with Department of Electrical and Computer Engineering and ElectroScience Laboratory, The Ohio State University, Columbus, OH 43210 USA (e-mail: frankford.7@osu.edu; johnson@ece.osu.edu).

E. Ertin is with Department of Electrical and Computer Engineering, The Ohio State University, Columbus, OH 43210 USA (e-mail: ertin.1@osu.edu).

Color versions of one or more of the figures in this paper are available online at http://ieeexplore.ieee.org.

Digital Object Identifier 10.1109/LSP.2010.2048138

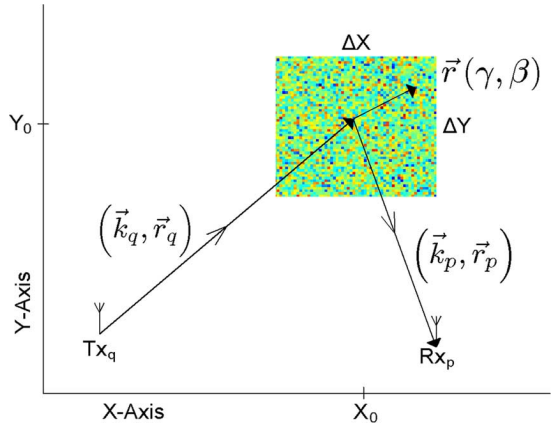

Fig. 1. Bistatic scattering from a rectangular target of size ΔX by ΔY. The antennas are assumed to be in the far field of the target.

requires that the spatial covariance of the target point scatterers $E\{\Sigma(\gamma,\beta)\Sigma^*(\gamma',\beta')\}$ be specified.

In [1]n the target point scatterers are spatially uncorrelated, so $E\{\Sigma(\gamma,\beta)\Sigma^*(\gamma',\beta')\}$ is defined as

$$E\{\Sigma(\gamma,\beta)\Sigma^*(\gamma',\beta')\} = \frac{1}{\Delta x\Delta y}\delta(\gamma-\gamma')\delta(\beta-\beta') \quad (2)$$

where the factor of one over the target area ensures that the total target "energy" is independent of its size. Correlation among the random scatterers is introduced by modifying (2) to

$$E\{\Sigma(\gamma,\beta)\Sigma^*(\gamma',\beta')\} = \frac{1}{\Delta x\Delta y}\frac{1}{2\pi C_d^2} \times \exp\left(\frac{-\left((\gamma-\gamma')^2+(\beta-\beta')^2\right)}{2C_d^2}\right) \quad (3)$$

where an azimuthally symmetric Gaussian correlation function has been chosen as a direct extension of (2). The parameter C_d is a correlation length: as C_d approaches zero, the point scatterers in the target become fully uncorrelated, and (2) is recovered. As C_d is increased, the point scatterer amplitudes are correlated over larger distances. The Gaussian correlation function does not guarantee that the integration of Σ over the target area yields unity, unless C_d is significantly less than the target dimensions. This difference is accounted for by a normalization in Section IV.

The entries in the covariance matrix $\boldsymbol{A}$ can be calculated from (1) and (3), resulting in (4):

$$E\{\alpha_{pq}\alpha_{st}^*\} = \frac{e^{-j(\vec{k}_p\cdot\vec{r}_p+\vec{k}_q\cdot\vec{r}_q-\vec{k}_s\cdot\vec{r}_s-\vec{k}_t\cdot\vec{r}_t)}}{2\pi C_d^2(\Delta X\Delta Y)} \cdot \int_{-\frac{\Delta X}{2}}^{\frac{\Delta X}{2}}\int_{-\frac{\Delta X}{2}}^{\frac{\Delta X}{2}} e^{\left(\frac{-(\gamma-\gamma')^2}{2C_d^2}\right)}e^{-j\left(p_x^{qp}\gamma-p_x^{ts}\gamma'\right)}d\gamma d\gamma' \times \int_{-\frac{\Delta Y}{2}}^{\frac{\Delta Y}{2}}\int_{-\frac{\Delta Y}{2}}^{\frac{\Delta Y}{2}} e^{\left(\frac{-(\beta-\beta')^2}{2C_d^2}\right)}e^{-j\left(p_y^{qp}\beta-p_y^{ts}\beta'\right)}d\beta d\beta'$$

$$\text{where } \vec{p}_{qp} = \vec{k}_q-\vec{k}_p = p_x^{qp}\hat{x}+p_y^{qp}\hat{y}$$
$$\text{and } \vec{p}_{ts} = \vec{k}_t-\vec{k}_s = p_x^{ts}\hat{x}+p_y^{ts}\hat{y}. \quad (4)$$

The two double integrals can each be transformed into a product of two single integrals by a rotation of coordinates, namely ($\gamma_d=\gamma-\gamma'$, $\gamma_s=\gamma+\gamma'$) and ($\beta_d=\beta-\beta'$, $\beta_s=\beta+\beta'$), where $d\gamma d\gamma' = d\gamma_d d\gamma_s/2$ and $d\beta d\beta' = d\beta_d d\beta_s/2$. Analytical solutions can then be found both for the diagonal ($p=s, q=t$) and off-diagonal entries of the covariance matrix through use of an integral table [8]. Both cases have the general form

$$E\{\alpha_{pq}\alpha_{st}^*\} = \frac{e^{-j(\vec{k}_p\cdot\vec{r}_p+\vec{k}_q\cdot\vec{r}_q-\vec{k}_s\cdot\vec{r}_s-\vec{k}_t\cdot\vec{r}_t)}}{2\pi(\Delta X\Delta Y)}F_xF_y \quad (5)$$

where F_x and F_y are functions of C_d and the geometry of the system. For diagonal entries, F_ν (where $\nu=x$ or y, and $\Delta\nu=\Delta X$ or ΔY) is

$$F_{\nu,\text{diag}} = 2C_d\text{Re}\left\{\sqrt{\frac{\pi}{2}}\left(\frac{\Delta\nu}{C_d}+jp_\nu^{qp}C_d\right)T\left(jp_\nu^{qp}C_d,\frac{\Delta\nu}{C_d}\right) + \exp\left(\frac{-\Delta\nu^2}{2C_d^2}\right)\cos\left(p_\nu^{qp}\Delta\nu\right)-1\right\} \quad (6)$$

and for off-diagonal entries:

$$F_{\nu,\text{off-diag}} = \left(\frac{\sqrt{2\pi}}{p_\nu^{qp}-p_\nu^{ts}}\right)\text{Im}\left\{e^{\left(\frac{j(p_\nu^{qp}-p_\nu^{ts})\Delta\nu}{2}\right)} \cdot\left[T\left(-jp_\nu^{ts}C_d,\frac{\Delta\nu}{C_d}\right)+T\left(jp_\nu^{qp}C_d,\frac{\Delta\nu}{C_d}\right)\right]\right\} \quad (7)$$

where

$$T(A,B) = e^{\frac{A^2}{2}}\left[\Phi\left(\frac{A+B}{\sqrt{2}}\right)-\Phi\left(\frac{A}{\sqrt{2}}\right)\right] \quad (8)$$

with the error function denoted by Φ evaluated for a complex argument [8]. The covariance matrix element amplitudes are now a function of the angular geometry (as included in p_ν^{qp} for example), the target sizes (ΔX, ΔY), and the correlation length C_d.

III. Scattering Behavior of a Correlated Target

In the case of the uncorrelated target, it was shown by [1] that the diagonal terms of $\boldsymbol{A}$ were unity, while the off-diagonal terms were negligibly small for spatially diverse antennas. This implies that each pair of antennas receives on average an equal amount of scattered power from the target ($E\{|\alpha_{pq}|^2\}$) and that the received fields are uncorrelated ($E\{\alpha_{pq}\alpha_{st}^*\}\approx 0$). However, if target spatial correlations are introduced, these conclusions are no longer true.

Fig. 2 shows the normalized bistatic scattering pattern, or $E\{|\alpha_{pq}|^2\}$, as a function of the angle between transmitter q and receiver p, of a $3\lambda\times 3\lambda$ target. When $C_d=0\lambda$, as is the case in Fig. 2(a), the pattern is uniform as expected. However, for $C_d=2\lambda$ [Fig. 2(b)], the target has a tendency to scatter power in the forward direction. Therefore, the amplitudes of the diagonal elements of $\boldsymbol{A}$ become dependent on the locations of the transmitters and receivers. A tendency to scatter in the forward direction by complex targets has been previously demonstrated through both numerical simulation [9] and experimental measurement [10].

To study the amount of correlation in the received fields due to spatially correlated scatterers, a target is placed at the origin and a co-located transmitter and receiver observe the target at 0°

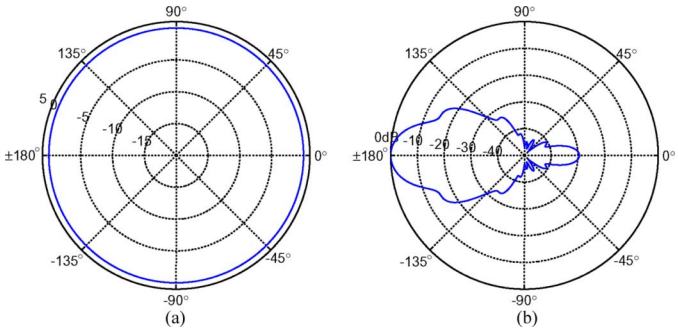

Fig. 2. Normalized bistatic scattering patterns in dB. (a) $C_d = 0\lambda$; (b) $C_d = 2\lambda$.

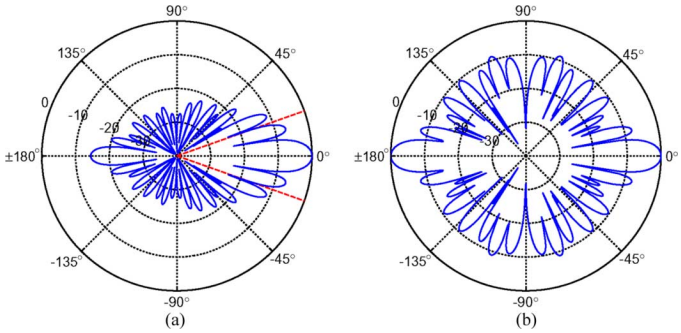

Fig. 3. Normalized covariance in dB of two monostatic transmitter and receiver pairs as a function of the difference in observation angle. (a) $C_d = 0\lambda$; (b) $C_d = 2\lambda$.

incidence. A second co-located transmitter and receiver pair is moved in a circle about the target, and $E\{\alpha_{pq}\alpha_{st}^*\}$ is calculated as a function of the angle between the monostatic pairs. Fig. 3 plots the resulting normalized magnitude of $E\{\alpha_{pq}\alpha_{st}^*\}$ versus the angle between the two monostatic radars. When $C_d = 0$, the covariance is maximum when the two monostatic pairs are close to one another in angle, and decreases as the angular separation increases. Equation (16) in [1] applied to this geometry shows than an angular separation of approximately 20° [marked by dashed lines in Fig. 3(a)] is required to achieve approximately independent observations. Increasing C_d tends to increase the covariance in all directions, particularly the covariance between the monostatic returns when the two radars are 180° from each other as illustrated in Fig. 3(b), which uses $C_d = 2\lambda$.

IV. Detector Formulation

MIMO radar measurements are corrupted by thermal noise in the radar receivers; noise corrupted measurements are represented by the vector $\bar{x}$. In the investigation that follows, a fixed system signal-to-noise ratio (SNR) is assumed and is defined in [1] as the ratio of the average total received power (summed over all transmit-receive antenna pairs and neglecting thermal noise) to the average thermal noise power summed over N receivers. This results in

$$\mathrm{SNR} = \frac{\mathcal{E}}{\sigma_n^2}\left(\frac{\mathrm{trace}\boldsymbol{A}}{NM}\right) \tag{9}$$

where $\mathcal{E}$ is the total transmitted power (divided equally among the M transmit antennas), and σ_n^2 is the average thermal noise power in each receiver. The term in parenthesis ensures that the total "energy" of the target is normalized to unity.

The received signal vector has the form $\bar{x} = \bar{n}$ under $\mathcal{H}_0$ (no target), and $\bar{x} = \bar{\beta} + \bar{n}$ under $\mathcal{H}_1$ (target present), where $\bar{n} \sim \mathcal{CN}(0, \boldsymbol{I}_{MN})$ is an additive complex Gaussian vector that models receiver thermal noise contributions, and where a division of $\bar{x}$ by σ_n has been included. The vector $\bar{\beta} \sim \mathcal{CN}(0, \boldsymbol{B})$ is proportional to the received signal vector $\bar{\alpha}$ such that $\bar{\beta} = \sqrt{\mathcal{E}/M}(\bar{\alpha}/\sigma_n)$ with $\boldsymbol{B}$ defined in terms of $\boldsymbol{A}$ and the SNR as:

$$\boldsymbol{B} = N\,\mathrm{SNR}\frac{\boldsymbol{A}}{\mathrm{trace}\boldsymbol{A}}. \tag{10}$$

The detection problem reduces to testing the hypothesis of whether a given complex vector observation is drawn from a complex Gaussian distribution having a first ($\boldsymbol{I}_{MN}$) or a second ($\boldsymbol{M} = \boldsymbol{B} + \boldsymbol{I}_{MN}$) covariance matrix under the null and alternate hypothesis respectively. For problems with no unknown parameters, the likelihood ratio test (LRT) provides the optimal detector in the Neyman-Pearson sense. The LRT for this case reduces to [11]

$$\bar{x}^H \boldsymbol{Q}\bar{x} \underset{<\mathcal{H}_0}{>^{\mathcal{H}_1}} \delta \tag{11}$$

where $\boldsymbol{Q} = \boldsymbol{I}_{MN} - \boldsymbol{M}^{-1}$. Implementing this detector requires a-priori knowledge of $\boldsymbol{M}$, which implies knowledge of the target size, orientation, correlation distance, and SNR. Because such information is unlikely to be available, implementation of (11) is not expected in practice. However, the performance of this LRT detector is utilized to assess the applicability of the "energy detector" in equation (24) of [1] to the correlated target model.

Under the null hypothesis, the energy detector $\|\bar{x}\|^2$ is a scaled chi-square random variable such that $\|\bar{x}\|^2 \sim (1/2)\chi^2_{(2MN)}$, and the decision threshold δ can be set as a function of the probability of false alarm (P_{FA}) [1]. In order to calculate the probability of detection (P_D), the covariance matrix $\boldsymbol{M}$ is calculated for a known MIMO geometry and target properties using the analytic expressions for $E\{\bar{\alpha}\bar{\alpha}^H\}$ derived in Section II. Reference [7] provides a procedure for numerically computing P_D using the singular value decomposition (SVD) of $\boldsymbol{M}$ to create a random vector whose entries are uncorrelated.

Following [7], the final form for P_D is

$$P_D = \sum_{m=1}^{N}\sum_{n=1}^{\mu_m} A_{m,n}\lambda_m^{\mu_m - n + 1} e^{\frac{-\delta}{\lambda_m}} \sum_{p=0}^{\mu_m - n} \frac{\left(\frac{\delta}{\lambda_m}\right)^p}{p!} \tag{12}$$

where $A_{m,n}$ are the partial fraction expansion coefficients defined by [7, eq. (10)], λ_m is the m^{th} eigenvalue of $\boldsymbol{M}$, μ_m is the algebraic multiplicity of λ_m, and δ is the decision threshold calculated as a function of P_{FA}.

V. Results

Fig. 4 illustrates a representative MIMO geometry with $M \times N = 2 \times 4$ for which the probability of detection was calculated for targets with varying degrees of spatial correlation. The rectangular target has $\Delta X = \Delta Y = 3\lambda$. This configuration satisfies the conditions derived in [1] for the covariance matrix to be approximately diagonal in the uncorrelated target case.

The probability of a missed detection ($P_{MD} = 1 - P_D$) for both the energy detector and the LRT (quadratic) detector is

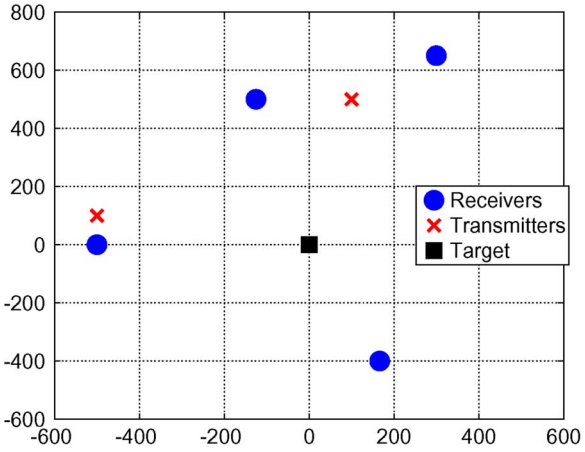

Fig. 4. MIMO geometry with $M = 2$ transmitters and $N = 4$ receivers spaced around a target located at the origin. The units of the X and Y coordinates are in wavelengths λ.

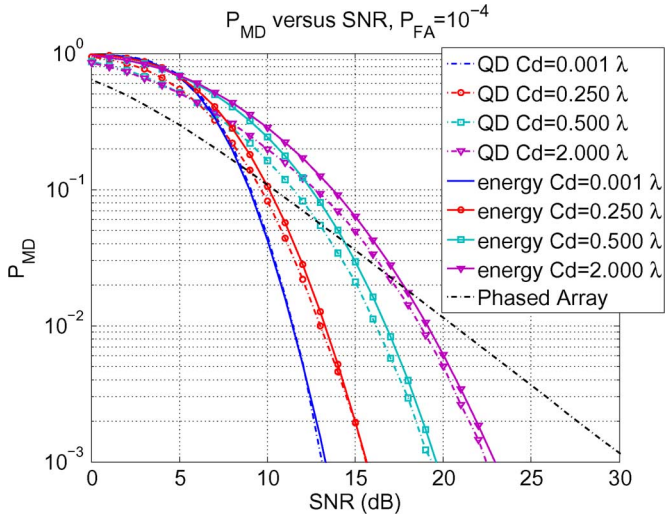

Fig. 5. Probability of missed detection for both the LRT detector (QD) and the energy detector (energy) for $P_{FA} = 10^{-4}$.

shown on a log scale in Fig. 5. This result, which depends on the closed form expression for the covariance matrix, has been independently verified through Monte Carlo simulations as well. For comparison, [1] also derives the probability of detection for a phased array system, and the reader is directed to the reference for details. The P_{MD} with both the energy detector and LRT (quadratic) detector for $C_d = 0.001$ agree closely with the uncorrelated scatterers case presented by Fishler *et al.* modified for $P_{FA} = 10^{-4}$. As the correlation is increased from zero to $C_d = 2\lambda$, the performance of the system decreases such that the SNR required for the MIMO radar to outperform the phased array increases by approximately 10 dB. These results suggest that the uncorrelated target model represents a best case scenario for evaluating the performance of a MIMO system using the energy detector.

Fig. 5 also compares the P_{MD} performance of the energy and LRT quadratic detectors for $P_{FA} = 10^{-4}$. As expected, the two perform identically in the uncorrelated target case. However, the performance of the LRT detector is only slightly better than the energy detector derived for the uncorrelated target case even for targets consisting of correlated scatterers.

VI. Conclusions

A correlated target scattering model was introduced in order to assess the impact of target spatial correlations on the MIMO detection algorithm derived for uncorrelated targets in [1]. A closed form solution for the covariance matrix $E\{\bar{\alpha}\bar{\alpha}^H\}$ was derived that can be calculated for any arbitrary MIMO geometry and level of target correlation. The energy detector derived in [1] for the uncorrelated target model was applied to the correlated target problem and was shown to have a similar performance to the optimal detector. Since the energy detector does not require prior knowledge of target properties, it is the preferred detector in this case. The MIMO system appears to perform best for uncorrelated targets, for which the bistatic scattering pattern is uniform in all directions, with decreasing performance for increasing correlation in the target. Further analysis of the target model presented is in progress to assess the degree to which this approach can describe scattering properties of realistic targets.

References

[1] E. Fishler, A. Haimovich, R. Blum, L. Cimini, D. Chizhik, and R. Valenzuela, "Spatial diversity in radars-models and detection performance," *IEEE Trans. Signal Process.*, vol. 54, no. 3, pp. 823–838, Mar. 2006.

[2] E. Fishler, A. Haimovich, R. Blum, D. Chizhik, L. Cimini, and R. Valenzuela, "MIMO radar: An idea whose time has come," in *Proc. IEEE Radar Conf.*, Apr. 2004, pp. 71–78.

[3] E. Fishler, A. Haimovich, R. Blum, L. Cimini, D. Chizhik, and R. Valenzuela, "Performance of MIMO radar systems: Advantages of angular diversity," in *Conf. Rec. Thirty-Eighth Asilomar Conf. Signals, Systems and Computers*, Nov. 2004, vol. 1, pp. 305–309.

[4] D. Rabideau and P. Parker, "Ubiquitous MIMO multifunction digital array radar," in *Conf. Rec. Thirty-Seventh Asilomar Conf. Signals, Systems and Computers*, Nov. 2003, vol. 1, pp. 1057–1064.

[5] D. Kirk, J. Bergin, P. Techau, and J. D. Carlos, "Multi-static coherent sparse aperture approach to precision target detection and engagement," in *2005 IEEE Int. Radar Conf.*, May 2005, pp. 579–584.

[6] N. H. Lehmann, A. M. Haimovich, R. S. Blum, and L. Cimini, "High resolution capabilities of MIMO radar," in *Fortieth Asilomar Conf. Signals, Systems and Computers*, Oct.–Nov. 2006, pp. 25–30.

[7] C. Du, J. S. Thompson, and Y. Petillot, "Predicted detection performance of MIMO radar," *IEEE Signal Process. Lett.*, vol. 15, pp. 83–86, 2008.

[8] I. Gradshteyn and I. Ryzhik, *Table of Integrals, Series, and Products*, 6th ed. New York: Academic, 2000, ch. 3, 8, pp. 333, 880.

[9] J. I. Glaser, "Bistatic RCS of complex objects near forward scatter," *IEEE Trans. Aerosp. Electron. Syst.*, vol. AES-21, no. 1, pp. 70–78, Jan. 1985.

[10] Y. S. Chesnokov and M. V. Krutikov, "Bistatic RCS of aircrafts at the forward scattering," in *Proc. CIE Int. Conf. Radar*, Oct. 1996, pp. 156–159.

[11] H. V. Poor, *An Introduction to Signal Detection and Estimation*, 2nd ed. Berlin, Germany: Springer-Verlag, 1994.